ELSEVIER

Physica B 308–310 (2001) 625–628

PHYSICA B

www.elsevier.com/locate/physb

The annealing product of the silicon vacancy in 6H–SiC

Th. Lingner[a,*], S. Greulich-Weber[a], J.-M. Spaeth[a], U. Gerstmann[b], E. Rauls[b], H. Overhof[b]

[a] *FB6-Experimental Physics, University of Paderborn, Warburgerstrasse 100, D-33098 Paderborn, Germany*
[b] *Theoretical Physics, University of Paderborn, Warburgerstrasse 100, D-33098 Paderborn, Germany*

Abstract

Radiation-induced defects in 6H-silicon carbide were investigated with electron paramagnetic resonance (EPR), the magnetic circular dichroism of the absorption (MCDA) and MCDA-detected EPR (MCDA-EPR). In irradiated samples, annealed beyond the annealing temperature of the isolated silicon vacancy (V_{Si}), we observed photo-EPR spectra of spin $S = 1$ centers, having the symmetry of nearest neighbor pair defects. By MCDA-EPR, they were associated to optical transitions with photon energies between 999 and 1075 meV. The hyperfine structure of the EPR spectra shows the presence of one single carbon and several silicon ligands. The experimental results are interpreted with the help of total energy and spin density data obtained from the standard local-density approximation of the density-functional theory, using relaxed defect geometries obtained from the self-consistent charge density-functional theory based tight binding scheme. The only model that explains all experimental findings is the photo-excited spin triplet state of the carbon antisite–carbon vacancy pair (C_{Si}–V_C) in the doubly positive charge state. We conclude that the C_{Si}–V_C defect is formed from V_{Si} as an annealing product by the movement of a carbon neighbor into the vacancy.

Keywords: Silicon carbide; Vacancies; Antisite; Electron paramagnetic resonance

1. Introduction

The silicon vacancy (V_{Si}) is a basic defect in silicon carbide (SiC) which can be introduced during crystal growth or by irradiation with high-energy particles, e.g. during ion implantation. The negatively charged V_{Si} has been identified by electron paramagnetic resonance (EPR). It anneals out at 750°C with an activation energy of 2.2 ± 0.3 eV [1]. In elemental semiconductors, a lattice vacancy can anneal out by moving through the lattice. In a compound semiconductor like SiC, the situation is more complicated, because chains of antisite defects must be created if the vacancy moves by nearest neighbor hops. It has recently been proposed that the first step in such an annealing process, the transformation of V_{Si} into the C_{Si}–V_C antisite-vacancy pair, is a quite probable process [2]. Here, we provide experimental evidence for the presence of the pair after annealing.

2. Experimental

The nitrogen-doped (10^{18} cm^{-3}) 6H–SiC samples were grown by the sublimation sandwich method. They were irradiated with reactor neutrons at a dose of 2×10^{18} cm^{-2} and then annealed for 2 min at 600°C, 1000°C and 1200°C, respectively. One sample of the same batch was left unirradiated, and another sample was irradiated but not annealed. EPR was measured with X-band (9.8 GHz) at 7 K. The samples were illuminated in situ with the light of a halogen lamp. The paramagnetic part of the magnetic circular dichroism (MCDA) is proportional to the spin polarization of the ground state of the optical transition. Saturating

*Corresponding author. Tel.: +49-5251-60-2749; fax: +49-5251-60-3247.
E-mail address: lingner@physik.uni-paderborn.de (T. Lingner).

0921-4526/01/$ - see front matter
PII: S0921-4526(01)00762-1

EPR transitions change the spin polarization which is observed as a decrease of the MCDA signal intensity (MCDA-EPR).

3. Computational

We used the self-consistent linear muffin-tin orbitals method in the atomic spheres approximation (LMTO-ASA), treating exchange and correlation effects within the framework of the local spin density approximation of the density-functional theory (LSDA-DFT) [3]. The atomic positions of the relaxed structure were obtained from additional calculations within the self-consistent charge density-functional theory based tight-binding (SCC-DFTB) scheme [4]. In a $(5\times6\times1)$ supercell model of the 6H polytype containing 300 atoms, the defect and its nearest and next nearest neighbors were relaxed. The relaxation energies were added to the LMTO total energies. Starting from the relaxed structures obtained from SCC-DFTB, the hyperfine (HF) interactions were calculated within an extended version of the LMTO-ASA Green's function method. For further details of this combined approach, see also Ref. [5].

4. Results and discussion

The EPR signal of neutron-irradiated and annealed 6H–SiC consists of six spin-triplet spectra. The angular dependence (Fig. 1) was analyzed using the usual spin Hamiltonian for $S=1$ including fine structure (Table 1). For three of the centers (P6a, b and c), the principal axis **z** of the fine structure tensor is parallel to the **c**-axis of the crystal (axial orientations). The **z**-axis of the other three centers (P7a, b and c) is oriented in the six $\{1\,1\,\bar{2}\,0\}$ planes at an angle θ to the **c**-axis (basal orientations). The angle θ is close to the ideal tetrahedral angle (70.529°). The letters a, b and c denote three different spectra of each orientation, which are thought to arise from the defect at the three inequivalent lattice sites in 6H–SiC. Similar spectra have been measured by EPR [6] and PL-EPR [7], but only two lattice sites have been identified so far [7].

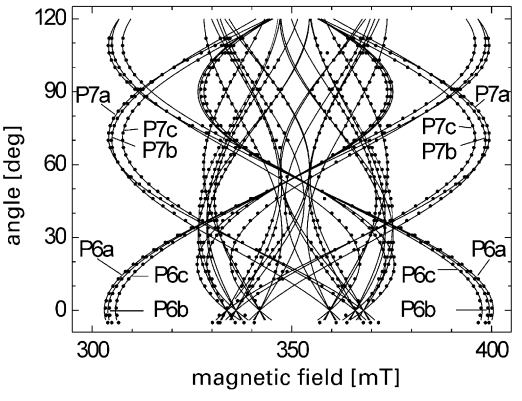

Fig. 1. Angular dependence of the P6/P7 EPR-spectra in 6H–SiC, measured at $T=7$ K in X-band (9.87 GHz). Dots indicate the experimental data. The solid lines are calculated curves using the parameters given in Table 1.

Table 1
EPR parameters, angle θ between the principal axis of the fine structure tensor and the **c**-axis, and optical transition energies of the P6/P7 centers[a]

Center	g	D (10^{-4} cm^{-1})	E (10^{-4} cm^{-1})	θ (deg)	hv (meV)
P6a	2.003	456	0	0	1075
P6b	2.003	447	0	0	1048
P6c	2.003	430	0	0	1011
P7a	2.003	449	−4	71.2	1049
P7b	2.003	441	46	70.0	1030
P7c	2.003	416	−1	70.5	999

[a] The notations P6 and P7 for the axial ($\theta=0°$) and the basal ($\theta\approx71°$) orientations is adopted from Ref. [6]. D is axially symmetric, E the anisotropic fine structure constant [9].

The P6/P7 spectra were present in the samples annealed at 600°C, 1000°C and 1200°C. Their highest intensity was observed after a 1000°C anneal. They were not found in the unannealed and in the unirradiated samples. All EPR spectra emerged only during illumination with photon energies above 1.1 ± 0.1 eV and hence, belong to a photo-excited state.

The MCDA and photoluminescence (PL) spectra of the unannealed and the 600°C-annealed sample showed optical transitions of the V_{Si}-related defect reported in Ref. [8]. This signal is absent after a 1000°C anneal. Instead, MCDA lines between 1 and 1.1 eV are observed (Fig. 2). In each of these MCDA lines, a single EPR spectrum from Table 1 was detectable with MCDA-EPR. The higher the value of D, the larger is the photon energy of the optical transition observed.

The HF splitting of the P6c EPR signal (Fig. 3) indicates the presence of one single ^{13}C nucleus ($A_\parallel=48$ MHz, intensity of one HF line $0.7\pm0.2\%$ of the central line) and four to eight ^{29}Si neighbors ($A_\parallel=12$ MHz, intensity $15\pm5\%$ of the central line). The ^{29}Si-related HF lines are broadened and may contain contributions from different Si neighbor shells with similar HF constants.

The symmetry characteristic for a nearest neighbor pair defect and the intrinsic nature of the defect, limit the possible models to the vacancy pair (V_{Si}–V_C), the antisite pair (C_{Si}–Si_C) and the vacancy–antisite pairs

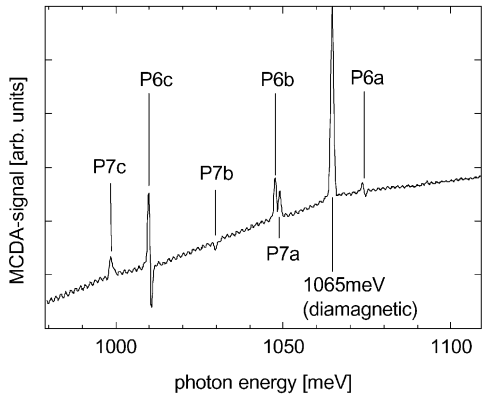

Fig. 2. MCDA spectrum of neutron-irradiated and at $T_{ann} = 1000°C$-annealed 6H–SiC, measured under additional excitation of the sample with an Ar-ion laser. In each of the P6/P7 MCDA lines, one of the EPR spectra from Table 1 was measured with MCDA-EPR.

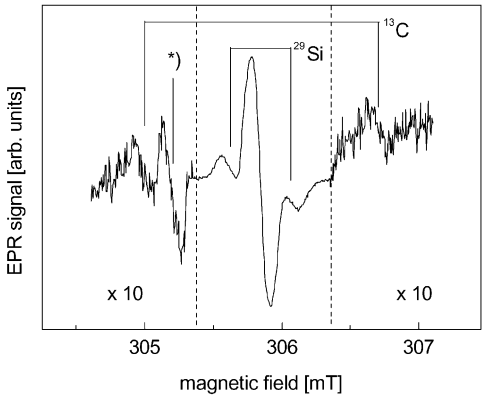

Fig. 3. Hyperfine structure of the P6c low field line for $\mathbf{B}\|\mathbf{c}$. The line marked with an asterisk belongs to a different defect.

V_{Si}–Si_C and C_{Si}–V_C. Only C_{Si}–Si_C and C_{Si}–V_C have one prominent C nucleus. The antisite pair C_{Si}–Si_C has excitation energies <0.2 eV and can, therefore, by no means explain the optical transitions of the P6/P7 centers (~ 1 eV).

The formation energy of C_{Si}–V_C is lower than that of V_{Si} for most charge states (Fig. 4). The calculated energy barrier for the formation of $(C_{Si}–V_C)^0$ from V_{Si}^0 (1.7 eV, [2]) is close to the experimentally observed activation energy for the annealing of V_{Si}^- (2.2 ± 0.3 eV, [1]). C_{Si}–V_C is, therefore, expected to be formed from V_{Si} as an annealing product.

In C_{3v} symmetry, C_{Si}–V_C has an $a_1(s)$ level in the valence band, an $a_1(p)$ and an e(p) level in the band gap (Fig. 5). The ground state of $(C_{Si}–V_C)^{2+}$ is a singlet $^1A_1$ ($a_1(s)\uparrow\downarrow$). Photon energies above 1.15 eV (exp.: 1.1 eV)

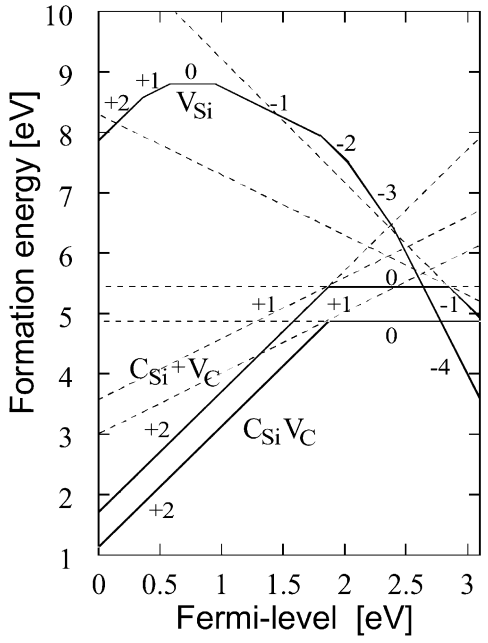

Fig. 4. Formation energies of the silicon vacancy (V_{Si}), the carbon–antisite carbon–vacancy pair ($C_{Si}V_c$), and sum of formation energies of the isolated carbon antisite and the isolated carbon vacancy ($C_{Si} + V_C$).

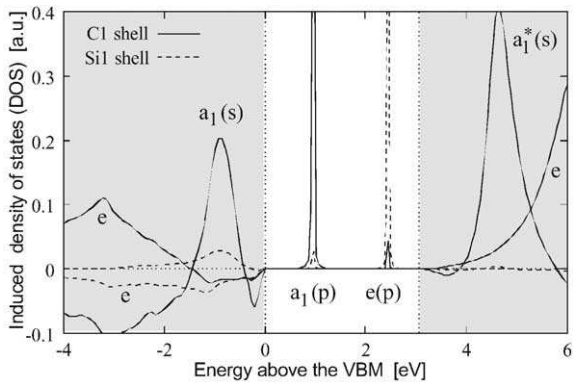

Fig. 5. Induced density of states for the diamagnetic ground state of the C_{Si}–V_C pair in the charge state $+2$.

can excite one electron from the $a_1(s)$ level into the $a_1(p)$ level, forming the $^1A_2$ ($a_1(s)\uparrow a_1(p)\downarrow$) state. A non-radiative transition to the energetically lower metastable triplet state $^3A_2$ ($a_1(s)\uparrow a_1(p)\uparrow$) is possible with help of phonons. This $^3A_2$ state gives rise to the P6/P7 EPR spectra observed experimentally. The MCDA is explained by the excitation of the $a_1(p)$ electron into the e(p) state ($a_1(s)\uparrow e(p)\uparrow$). The calculated photon energy (1.52 eV) is in reasonable agreement with the experimental values (1.0–1.1 eV).

The calculated HF interaction with the C_{Si} approaches the experimental value when C_{Si} relaxes 22% away from V_C. This is close to the relaxation predicted by SCC-DFTB (16%). The three Si neighbors of V_C and three next nearest neighbors of C_{Si} (in the direction of the defect axis) contribute to the silicon HF interaction with similar constants, explaining the observed HF lines (6 ± 2 inequivalent Si nuclei).

A similar excitation scheme as for $(C_{Si}–V_C)^{2+}$ is possible for $(C_{Si}–V_C)^0$, but, in this case, the e(p) state is occupied in the metastable triplet state ^3E ($a_1(s)\uparrow\downarrow a_1(p)\uparrow e(p)\uparrow$) and gives rise to a large HF interaction with the Si neighbors of V_C (>150 MHz), which, by far, exceeds the experimentally observed value. Thus, this charge state must be ruled out. For a more detailed discussion, see Ref. [5].

In summary, we have identified the $C_{Si}–V_C$ pair in 6H–SiC in the doubly positive charge state on all inequivalent lattice sites and in all orientations. The $C_{Si}–V_C$ pair is the ideal candidate for the annealing product of V_{Si}. The bad news, though, is that the $C_{Si}–V_C$ defect is electrically and optically active. It has a charge transfer level just above midgap. Thus, at least a second anneal step is required to remove the electrical activity of silicon vacancy-related defects.

References

[1] H. Itoh, M. Yoshikawa, I. Nashiyama, S. Misawa, H. Okumura, S. Yoshida, IEEE Trans. Nucl. Sci. 37 (1990) 1732.
[2] E. Rauls, Th. Lingner, Z. Hajnal, S. Greulich-Weber, Th. Frauenheim, J.-M. Spaeth, Phys. Stat. Sol. B 217/2 (2000) R1.
[3] O. Gunnarsson, O. Jepsen, O.K. Andersen, Phys. Rev. B 27 (1983) 7144.
[4] Th. Frauenheim, et al., Phys. Stat. Sol. B 217 (2000) 41.
[5] Th. Lingner, S. Greulich-Weber, J.-M. Spaeth, U. Gerstmann, H. Overhof, E. Rauls, Z. Hajnal, Th. Frauenheim, Phys. Rev. B, submitted for publication.
[6] V.S. Vainer, V.A. Il'in, Sov. Phys. Sol. State 23 (1981) 2126.
[7] N.T. Son, P.N. Hai, M. Wagner, W.M. Chen, A. Ellison, C. Hallin, B. Monemar, E. Janzén, Semicond. Sci. Technol. 14 (1999) 1141.
[8] E. Sörman, N.T. Son, W.M. Chen, O. Kordina, C. Hallin, E. Janzén, Phys. Rev. B 61 (2000) 2613.
[9] J.-M. Spaeth, J.R. Niklas, R.H. Bartram, Structural Analysis of Point Defects in Solids, Solid State Sciences 43, Springer, Heidelberg, 1992.